

## RESEARCH ARTICLE



# Ultra-sensitive Photonic Crystal Fiber Based Refractive Index Sensor for Efficient Alcohol Detection at Near Infrared Region

Amit Halder<sup>1,2,\*</sup>, Md Riyad Tanshen<sup>2</sup>, Md Mushfiqur Rahman Neidhe<sup>2</sup> and Md Mohsin<sup>2</sup>

<sup>1</sup>Department of Electrical and Electronic Engineering, Rajshahi University of Engineering and Technology, Bangladesh

<sup>2</sup>Department of Electrical and Electronic Engineering, World University of Bangladesh, Bangladesh

**Abstract:** This paper describes the development and evaluation of an ultra-sensitive modified circular photonic crystal fiber (MC-PCF) sensor for efficient alcohol detection. Operating at 850 nm, the sensor has exceptional relative sensitivity and low confinement losses, making it suitable for a wide range of practical applications. The MC-PCF sensor was developed using COMSOL Multiphysics and a finite element method to improve light-matter interaction by increasing sensitivity and precision. Performance metrics such as relative sensitivity, confinement loss, and nonlinear coefficients were assessed for various alcohols (methanol, ethanol, propanol, butanol, and pentanol). The sensor has impressive relative sensitivity values: 95.51% for methanol, 97.2% for ethanol, 97.85% for propanol, 98.69% for butanol, and 99.4% for pentanol. The confinement losses are  $2.345 \times 10^{-9}$ ,  $1.022 \times 10^{-9}$ ,  $8.656 \times 10^{-10}$ ,  $1.821 \times 10^{-9}$ , and  $3.097 \times 10^{-9}$  dB/m, respectively. Methanol, ethanol, propanol, butanol, and pentanol have nonlinear coefficients of 78.95, 75, 73.69, 73.03, and 72.54  $W^{-1}km^{-1}$ , respectively. The numerical apertures for the MC-PCF sensor at an 850 nm operating wavelength are 0.2599 for methanol, 0.2566 for ethanol, and 0.2567 for propanol, butanol, and pentanol. The optimized design of the MC-PCF sensor significantly improves light-matter interaction, resulting in high precision and rapid response when detecting changes in alcohol concentration. This makes the proposed sensor a strong and dependable solution for industrial quality control, medical diagnostics, and environmental monitoring. In summary, the MC-PCF sensor's outstanding sensitivity and low confinement loss at the near-infrared region demonstrate its potential for effective alcohol detection across various fields.

**Keywords:** modified circular photonic crystal fiber, alcohol detection sensor, relative sensitivity, confinement loss, light-matter interaction

## 1. Introduction

The detection and quantification of alcohol concentration are pivotal in diverse fields such as industrial quality control, medical diagnostics, and environmental monitoring [1]. Conventional methods like gas chromatography and mass spectrometry, while precise, are often cumbersome and costly and require elaborate sample preparation [2]. In contrast, optical fiber sensors offer a promising alternative due to their high sensitivity, rapid response, and capability for real-time monitoring [3]. Photonic crystal fibers (PCFs) are a unique class of optical fibers characterized by their periodic microstructure, which runs along their length and enables precise control over light propagation [4]. This distinctive design can be tailored to amplify the interaction between light and the analyte, thereby enhancing the sensor's sensitivity. This study introduces an ultra-sensitive PCF sensor specifically optimized for efficient alcohol detection at an operating wavelength of 850 nm. The sensor exploits the refractive index variations induced by different alcohol

concentrations, achieving high sensitivity and specificity. Recent advancements in PCF sensors have significantly improved the detection of alcohols in applications such as industrial quality control, medical diagnostics, and environmental monitoring [5]. PCF sensors operating in the near-infrared (NIR) region are particularly effective due to their capability to confine light within a small core, enhancing light-matter interactions and increasing sensitivity [6]. The development of PCF sensors for alcohol detection has gained significant traction over the past decade, driven by their high sensitivity and ability to operate over a wide range of wavelengths. Early studies laid the groundwork for using PCFs to improve alcohol detection accuracy in industrial, medical, and environmental applications. In 2017, Islam et al. [7] introduced a Zeonex-based PCF for alcohol detection in the terahertz frequency range. This design achieved 88.6% sensitivity with a very low confinement loss, demonstrating the potential of PCF sensors in detecting alcohol in beverages through a simple, easily fabricated structure [7]. Islam et al. [8] proposed a hexagonal PCF (H-PCF) with a specific geometric arrangement of core holes was numerically analyzed using the finite element method (FEM), demonstrating a sensitivity of 53.22% for ethanol detection at a wavelength of 1.33  $\mu m$ , highlighting its effectiveness in chemical sensing

\*Corresponding author: Amit Halder, Department of Electrical and Electronic Engineering, Rajshahi University of Engineering and Technology and Department of Electrical and Electronic Engineering, World University of Bangladesh, Bangladesh. Email: [amit.halder@eee.wub.edu.bd](mailto:amit.halder@eee.wub.edu.bd)

applications. Following this, Rahman et al. [9] further explored hollow-core PCF designs for beverage alcohol detection in the terahertz range, achieving 89.85% sensitivity with ultra-low confinement loss, highlighting the flexibility of PCF sensors in applications requiring precise alcohol concentration measurement. The exploration of PCF sensors continued in 2021 with Habib et al. [10], who proposed a hollow-core H-PCF for detecting commonly used alcohols such as methanol and ethanol. Their sensor achieved 89% relative sensitivity, emphasizing the utility of simple PCF designs that can be fabricated using existing technologies [10]. More recently, Shi et al. [11] developed a PCF sensor with elliptical core holes designed specifically for detecting propanol, butanol, and pentanol. Their sensor, operating at a wavelength range of 0.8 to 2.0  $\mu\text{m}$ , achieved sensitivities of 93.3% for propanol, 88.7% for butanol, and 82.2% for pentanol, with extremely low birefringence and confinement loss [11]. To achieve better refractive index sensing in the visible spectrum, Das et al. [12] presented an affordable technique utilizing chemically etched tapered telecommunication fibers combined with gold nanoparticles. Similarly, Liang et al. [13] showed that minute changes in refractive index can be detected using etch-eroded fiber Bragg gratings and Fabry-Pérot interferometers, with the latter providing a higher sensitivity because of its narrower spectral features. The potential of chemically treated and structurally altered optical fibers in creating extremely sensitive refractive index sensors is demonstrated by these studies taken together. The proposed ultra-sensitive modified circular PCF (MC-PCF) sensor presented in this study builds on these advancements by employing a modified circular design optimized for light-matter interaction using computational methods, achieving superior sensitivity (up to 99.4% for pentanol) and extremely low confinement losses (down to  $8.656 \times 10^{-10}$  dB/m), making it highly suitable for diverse applications. The study focuses on optimizing the PCF structure to maximize sensitivity to refractive index changes by adjusting the geometric parameters such as the core diameter and the arrangement of air holes. The resulting design significantly enhances light-matter interaction within the fiber. Experimental data

reveal relative sensitivities of 95.51% for methanol, 97.2% for ethanol, 97.85% for propanol, 98.69% for butanol, and 99.4% for pentanol. Furthermore, the confinement losses for these alcohols are extremely low, ensuring minimal signal attenuation. The nonlinear coefficients indicate the fiber's effectiveness in maintaining high performance across various alcohol types.

## 2. Methods

### 2.1. Design methodology

Finding the essential geometric parameters required to build the MC-PCF is the first step in the design process. Pitch ( $\Lambda$ ) and the relative air hole diameters ( $d_a$ ,  $d_1$ ,  $d_2$ ,  $d_3$ ,  $d_4$ , and  $d_5$ ), all normalized to pitch, are among these parameters. The core and cladding structure of the proposed PCF are shown in cross-section in Figure 1. The relative diameters in this design are as follows:  $d_a/\Lambda = 1.4$ ,  $d_1/\Lambda = d_2/\Lambda = d_4/\Lambda = 0.5$ ,  $d_3/\Lambda = 0.76$ , and  $d_5/\Lambda = 0.63$ . The pitch ( $\Lambda$ ) is set to 1.5  $\mu\text{m}$ . For analyte injection, the central air hole ( $d_a$ ) can hold alcohols like methanol, ethanol, propanol, butanol, and pentanol. The first ring's air holes are spaced 30 degrees apart, the second and third rings' air holes are spaced 15 degrees apart, and the fourth and fifth rings' air holes are spaced 7.5 degrees apart. A perfectly matched layer (PML) is applied in a circle around the perimeter of the structure, 10% of the cladding radius in thickness, to minimize reflection and backscattering [14]. Unwanted reflections are efficiently absorbed by this PML layer. The PML thickness in the suggested design is changed to 1  $\mu\text{m}$  using a scaling factor of 1. The fabrication of silica-based PCF for refractive index sensing typically involves a stack-and-draw process. Initially, silica rods are stacked to form a preform that defines the microstructure of the fiber, which is then drawn into the PCF through a fiber-drawing tower [15]. The proposed MC-PCF can also be fabricated using stack-and-draw method.

To employ PCFs for liquid sample sensing and photochemistry experiments, the sample needs to be pushed into

**Figure 1**  
Cross-sectional view of the proposed MC-PCF refractive index sensor

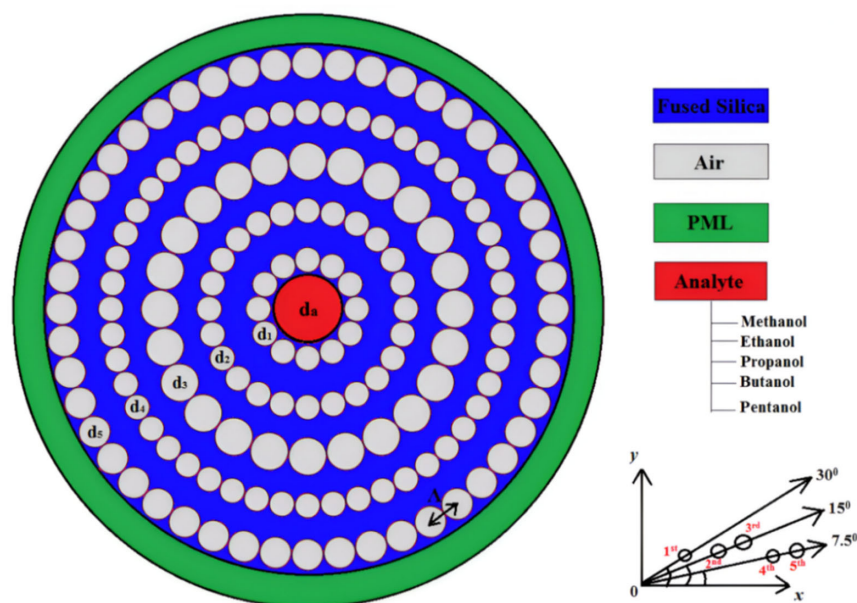
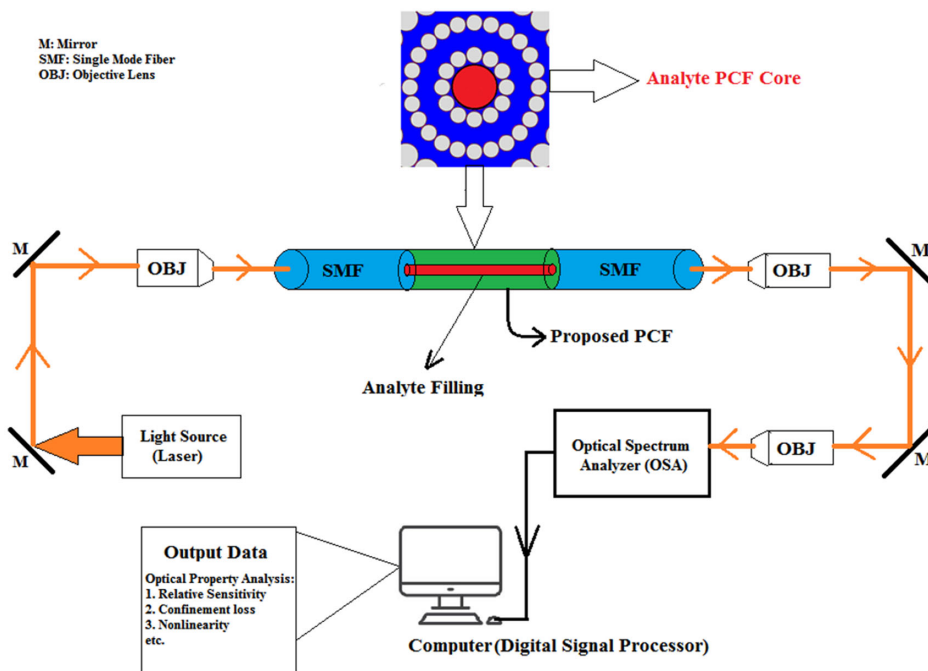


**Figure 2**  
Schematic representation of proposed MC-PCF refractive index sensor integrated photochemistry setup



the fiber’s holes. In this instance, the core air hole has been filled with the alcohol analyte sample. A schematic representation of a typical MC-PCF analyte refractive index sensor integrated photochemistry setup is shown in Figure 2. Figure 2 shows how a microscope objective lens with a corresponding numerical aperture (NA) is used to couple light into the core. The directions of the laser light entering the objective lens were changed using the mirrors (M). To analyze the optical properties of the injected alcohols, such as their effective area, relative sensitivity, power fraction, confinement loss, and effective mode index, the light laser is passed through the analytic MC-PCF core through single-mode fibers (SMF) and the optical spectrum analyzer (OSA) provides data to the computer. After that, the computer will display the data in a graphical and numerical format. An index-matching gel is used to connect the SMF to the PCF, guaranteeing effective light coupling with low loss. The analyte liquid does not fill the  $d_1$  to  $d_5$  air holes; they are only there to improve light confinement in the central hollow core. In the PCF diagram, the direction of light propagation is indicated by the orange arrow. The digital signal processor processes the spectral intensity data from the OSA output to further analyze the optical characteristics.

To ensure accurate representation, an improved meshing technique was utilized. For the proposed MC-PCF design in this simulation, the physics-controlled “fine” mesh parameter was employed. Figure 3 shows a one-fourth cross-sectional view of the fine mesh parameter used in the finite element analysis with COMSOL Multiphysics simulation software. This simulation analyzed a total of 52,486 elements using the “fine” mesh setting. The simulation process involved solving for 401,563 degrees of freedom. After 7 iterations with the eigenvalue solver, the error rate was reduced to  $5.9 \times 10^{-8}$ , resulting in high accuracy in data acquisition.

Table 1 provides the refractive index values for various alcohols at 850 nm, demonstrating a trend of increasing refractive index with the length of the alcohol-filled analyte core, from methanol to pentanol [16, 17].

**Figure 3**  
One-fourth cross-sectional meshing view of the proposed MC-PCF

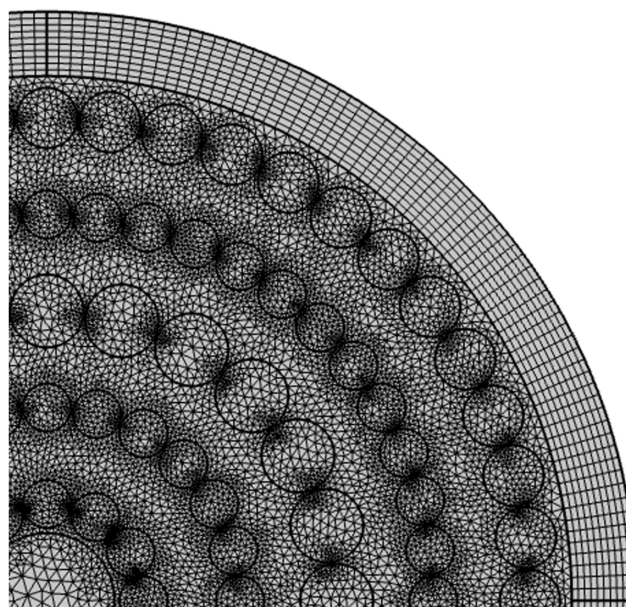


**Table 1**  
Refractive index table for alcohols at 850 nm

Alcohol	Chemical formula	Refractive index at 850 nm, 20°C
Methanol	CH <sub>3</sub> OH	1.3214
Ethanol	C <sub>2</sub> H <sub>5</sub> OH	1.3566
Propanol	C <sub>3</sub> H <sub>7</sub> OH	1.3798
Butanol	C <sub>4</sub> H <sub>9</sub> OH	1.3936
Pentanol	C <sub>5</sub> H <sub>11</sub> OH	1.4019

## 2.2. Numerical methodology

The modal properties of the proposed fiber were calculated using the COMSOL commercial full-vector finite element software. The core principle of light propagation in the MC-PCF sensor is governed by Maxwell's equations. For a time-harmonic electromagnetic wave in a dielectric medium, Maxwell's equations can be simplified to the Helmholtz wave equation [18]:

$$\nabla \times (\nabla \times \mathbf{E}) - k_0^2 n^2 \mathbf{E} = 0 \quad (1)$$

where  $\mathbf{E}$  is the electric field vector,  $k_0 = 2\pi/\lambda$  is the free-space wave number,  $n$  is the refractive index distribution of the material, and  $\lambda$  is the operating wavelength.

The Sellmeier equation is widely used to model the wavelength-dependent refractive index of transparent materials, including silica ( $\text{SiO}_2$ ). The Sellmeier equation for silica, which provides an accurate description of its refractive index in the visible and NIRs, is given by [19]:

$$n_{\text{SiO}_2}(\lambda) = \sqrt{1 + \frac{B_1 \lambda^2}{\lambda^2 - C_1} + \frac{B_2 \lambda^2}{\lambda^2 - C_2} + \frac{B_3 \lambda^2}{\lambda^2 - C_3}} \quad (2)$$

Where the coefficients for the Sellmeier equation for fused silica are given as follows:  $B_1 = 0.6961663$ ,  $B_2 = 0.4079426$ ,  $B_3 = 0.8974794$ ,  $C_1 = 4.67914826 \times 10^{-3} \mu\text{m}^2$ ,  $C_2 = 1.35120631 \times 10^{-2} \mu\text{m}^2$ , and  $C_3 = 97.9340025 \mu\text{m}^2$ .

The effective refractive index  $n_{\text{eff}}$  for a particular mode in the PCF is obtained from the eigenvalue analysis of the wave equation. The eigenvalue problem is formulated as [20]:

$$n_{\text{eff}} = \frac{\beta}{k_0} \quad (3)$$

where  $\beta$  is the propagation constant of the mode.

The power fraction provides insight into how much of the mode's power is confined within a desired region, which is crucial for optimizing the design and performance of optical fibers and waveguides. For a waveguide or fiber, the power fraction ( $f$ ) in a specific region (e.g., the core) can be defined as [21]:

$$f = \left( \frac{\int_{\text{core}} |\mathbf{E}|^2 dA}{\int_{\text{total}} |\mathbf{E}|^2 dA} \right) \times 100\% \quad (4)$$

where  $|\mathbf{E}|$  is the magnitude of the electric field intensity.

The relative sensitivity ( $r$ ) of a refractive index-based PCF sensor is a measure of the overlap of the guided mode with the analyte-filled air holes and is given by [22]:

$$r = \left( \frac{n_{\text{analyte}} \int_{\text{analyte}} |\mathbf{E}|^2 dA}{n_{\text{core}} \int_{\text{total}} |\mathbf{E}|^2 dA} \right) \times 100\% \quad (5)$$

where  $n_{\text{analyte}}$  is the refractive index of the analyte (methanol, ethanol, etc.),  $n_{\text{core}}$  is the refractive index of the core material,  $|\mathbf{E}|$  is the electric field intensity magnitude.

The confinement loss, which quantifies the power leakage from the core to the cladding, is expressed in terms of the imaginary part of the effective refractive index [23]:

$$L_c = \frac{8.686 \times 2\pi \times \text{Im}[n_{\text{eff}}]}{\lambda} \text{ dB/m} \quad (6)$$

where  $\text{Im}[n_{\text{eff}}]$  is the imaginary part of the effective refractive index and  $\lambda$  is the operating wavelength.

The nonlinear coefficient of a PCF, which is essential for nonlinear optical effects, is defined as [24]:

$$\gamma = \frac{2\pi n_2}{\lambda A_{\text{eff}}} \times 10^3 \text{ W}^{-1} \text{ km}^{-1} \quad (7)$$

where  $n_2$  is the nonlinear refractive index of the material,  $A_{\text{eff}}$  is the effective mode area of the guided light, calculated as [25]:

$$A_{\text{eff}} = \frac{[\iint |\mathbf{E}(x, y)|^2 dx dy]^2}{\iint |\mathbf{E}(x, y)|^4 dx dy} \mu\text{m}^2 \quad (8)$$

The NA of the MC-PCF sensor, which represents the fiber's ability to collect light, is given by [26]:

$$NA = \frac{1}{\sqrt{1 + \frac{\pi A_{\text{eff}}}{\lambda^2}}} \quad (9)$$

where  $A_{\text{eff}}$  is the effective area of the proposed fiber and  $\lambda$  is the operating wavelength.

## 3. Results and Discussion

This section presents the performance evaluation of the proposed MC-PCF sensor for alcohol detection, focusing on key metrics such as relative sensitivity, confinement loss, and nonlinear coefficients at an 850 nm wavelength. The findings demonstrate the sensor's superior sensitivity and low confinement loss compared to existing designs, highlighting its potential for applications in industrial quality control, medical diagnostics, and environmental monitoring [27, 28]. Figure 4 shows the

**Figure 4**  
Wavelength versus effective refractive index curve for different alcohol analytes using the MC-PCF refractive index sensor

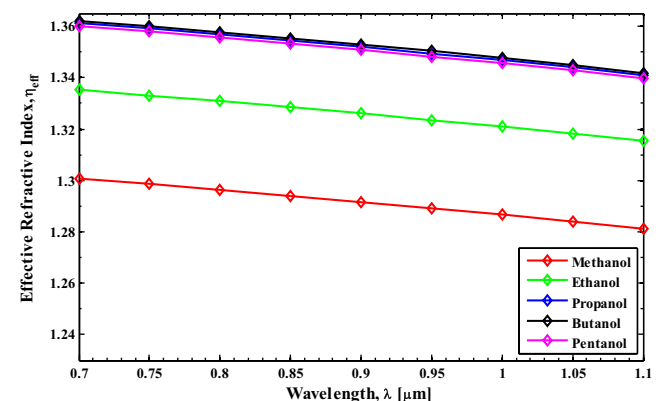
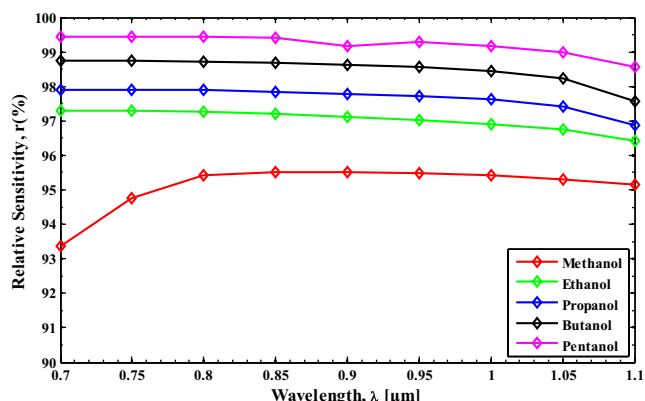


**Figure 5**  
Wavelength-dependent relative sensitivity curve for different alcohol analytes using the MC-PCF sensor

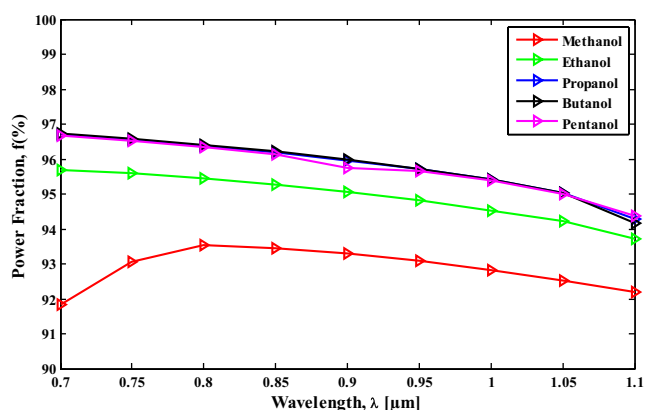


effective refractive index variations for different alcohol analytes (methanol, ethanol, propanol, butanol, and pentanol) at 850 nm, where the values are 1.294, 1.328, 1.355, 1.355, and 1.353, respectively. The increasing trend from methanol indicates the MC-PCF sensor's sensitivity to changes in the analyte's refractive index. However, the similar values for propanol, butanol, and pentanol suggest a saturation effect or reduced sensitivity for higher refractive indices. This highlights the need for optimizing the sensor design to better distinguish analytes with closely spaced refractive indices.

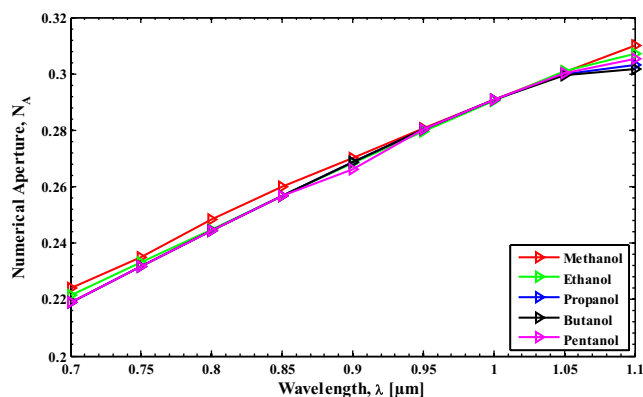
Figure 5 illustrates the wavelength-dependent relative sensitivity curve for different alcohol analytes, showing that at 850 nm, the sensor achieves relative sensitivities of 95.51% for methanol, 97.2% for ethanol, 97.85% for propanol, 98.69% for butanol, and 99.4% for pentanol. The increasing sensitivity trend with higher alcohols indicates the MC-PCF sensor's enhanced performance with analytes of higher refractive indices, making it highly effective for detecting subtle changes in the surrounding medium.

Figure 6 presents the wavelength versus power fraction curve for different alcohol analytes, where the power fractions at 850 nm are 93.45% for methanol, 95.26% for ethanol, 96.19% for propanol, 96.21% for butanol, and 96.15% for pentanol. The

**Figure 6**  
Wavelength versus power fraction curve for different alcohol analytes using the MC-PCF sensor



**Figure 7**  
Wavelength-dependent numerical aperture (NA) curves for different alcohol analytes

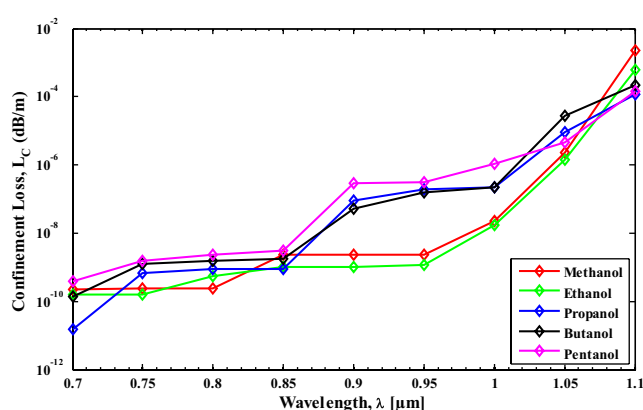


increase in power fraction from methanol to propanol indicates the sensor's capability to confine more light with higher refractive index analytes. The nearly identical values for propanol, butanol, and pentanol suggest a plateau effect, where further increases in the analyte refractive index have a minimal impact on the power fraction, highlighting the MC-PCF sensor's potential for stable sensing performance across a range of higher refractive index analytes.

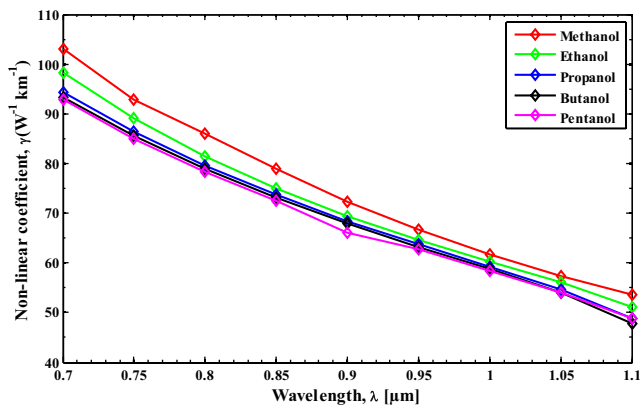
Figure 7 depicts the wavelength-dependent NA curve for different alcohol analytes, showing NA values of 0.2599 for methanol, 0.2566 for ethanol, and 0.2567 for propanol, butanol, and pentanol at 850 nm. The higher NA for methanol indicates better light-guiding ability compared to the other analytes, while the nearly identical values for propanol, butanol, and pentanol suggest minimal variation in the light acceptance angle for analytes with similar refractive indices.

Figure 8 presents the wavelength-dependent confinement loss curve for different alcohol analytes, with values at 850 nm of  $2.345 \times 10^{-9}$  dB/m for methanol,  $1.022 \times 10^{-9}$  dB/m for ethanol,  $8.656 \times 10^{-10}$  dB/m for propanol,  $1.821 \times 10^{-9}$  dB/m for butanol, and  $3.097 \times 10^{-9}$  dB/m for pentanol. The lowest confinement loss is observed for propanol, indicating superior light confinement, while methanol and pentanol exhibit higher

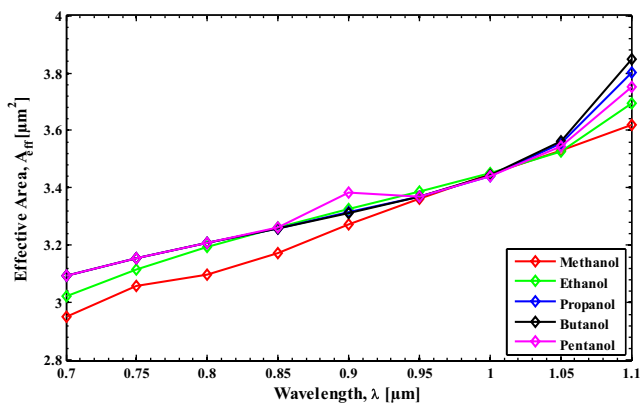
**Figure 8**  
Wavelength versus confinement loss curve for different alcohol analytes



**Figure 9**  
Wavelength versus nonlinear coefficient curve for different alcohol analytes



**Figure 10**  
Wavelength versus effective area curve for different alcohol analytes



losses. This variation highlights the MC-PCF sensor’s sensitivity to different alcohol analytes, with lower confinement losses suggesting better performance for specific analytes.

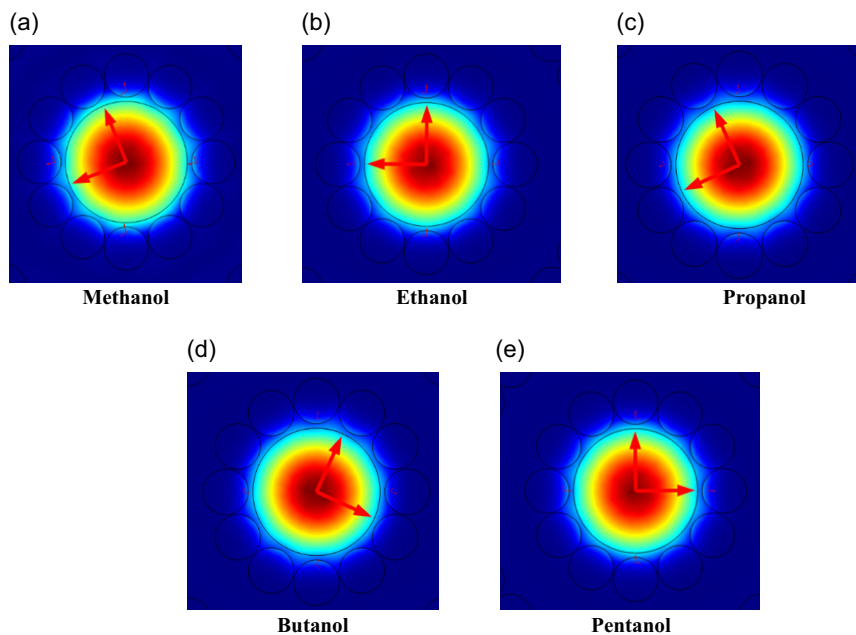
Figure 9 displays the wavelength versus nonlinear coefficient curve for various alcohol analytes at 850 nm, with nonlinear coefficients of 78.95, 75, 73.69, 73.03, and 72.54W<sup>-1</sup>km<sup>-1</sup> for methanol, ethanol, propanol, butanol, and pentanol, respectively. The observed decrease in the nonlinear coefficient with increasing analyte refractive index suggests that the MC-PCF’s nonlinear optical response diminishes as the refractive index rises. Methanol exhibits the highest nonlinear coefficient, indicating stronger nonlinear effects at lower refractive indices, while higher refractive index analytes show reduced nonlinearity.

Figure 10 illustrates the wavelength versus effective area curve for different alcohol analytes at 850 nm, with effective areas of 3.174 μm<sup>2</sup> for methanol, 3.262 μm<sup>2</sup> for ethanol, 3.26 μm<sup>2</sup> for propanol, 3.259 μm<sup>2</sup> for butanol, and 3.261 μm<sup>2</sup> for pentanol. The effective area shows minimal variation across the different alcohols, indicating that the sensor’s mode confinement is relatively stable regardless of the analyte’s refractive index. Methanol exhibits the smallest effective area, suggesting slightly better mode confinement, while the values for the other alcohols are very close, reflecting consistent performance of the MC-PCF sensor in terms of mode propagation and light guidance across the range of tested analytes.

Figure 11 shows the distribution of the fundamental mode electromagnetic field for the various analytes in the suggested MC-PCF. The suggested MC-PCF core’s polarization pattern and light compactness are depicted in the figure. The polarization direction of the electric field vectors in the fundamental mode is shown by the red arrows in Figure 11. By graphically depicting the electromagnetic field’s distribution within the core, these arrows aid in the illustration of the optical confinement and mode structure for various alcohol analytes.

In Table 2, we compare various PCF sensors for alcohol detection, highlighting differences in sensor designs, operating wavelengths, relative sensitivities, and confinement losses.

**Figure 11**  
Electromagnetic field distribution for different alcohol analytes



**Table 2**  
**Comparison of PCF sensors for alcohol detection, highlighting sensor designs, operating wavelengths, relative sensitivities, confinement losses, and applications**

References	Operating wavelength/ Frequency	Materials	Alcohol sensitivity	Confinement loss [dB/m]	Application
[7]	1.9 THz	Zeonex	Sensitivity: 88.6%	$3.15 \times 10^{-8}$	Alcohol detection in beverages
[8]	1.33 $\mu\text{m}$	Silica	Benzene: 55.56% Ethanol: 53.22% Water: 48.19%	N/A	Telecommunication, chemical sensing and bio-sensing
[9]	0.4–1.2 THz	Topas	Sensitivity: 89.85%	$8.686 \times 10^{-12}$	Alcohol detection in beverages
[10]	1.55 $\mu\text{m}$	Silica	Methanol: 75.22%, Ethanol: 82.52%, Propanol: 86.74% and Butanol: 88.34%,	Methanol: $3.29 \times 10^{-10}$ , Ethanol: $1.50 \times 10^{-10}$ , Propanol: $1.35 \times 10^{-10}$ , and Butanol: $9.33 \times 10^{-11}$	Alcohol detection in daily life
[11]	0.8–2.0 $\mu\text{m}$	Silica	Propanol: 93.3%, Butanol: 88.7%, Pentanol: 82.2%	Propanol: $9.80 \times 10^{-13}$ Butanol: $4.91 \times 10^{-13}$ Pentanol: $1.03 \times 10^{-13}$	Alcohol detection in beverages and medical applications
Proposed MC-PCF Sensor (Current Study)	850 nm	Silica	Methanol: 95.51, Ethanol: 97.2, Propanol: 97.85, Butanol: 98.69, Pentanol: 99.4	Methanol: $2.345 \times 10^{-9}$ , Ethanol: $1.022 \times 10^{-9}$ , Propanol: $8.656 \times 10^{-10}$ , Butanol: $1.821 \times 10^{-9}$ , Pentanol: $3.097 \times 10^{-9}$	Industrial quality control, medical diagnostics, environmental monitoring

#### 4. Conclusion

In conclusion, the developed MC-PCF sensor demonstrates exceptional performance for alcohol detection at 850 nm. The sensor's high relative sensitivity, ranging from 95.51% for methanol to 99.4% for pentanol, coupled with minimal confinement losses, highlights its effectiveness in detecting various alcohols with precision. The use of COMSOL Multiphysics and FEMs in the sensor design has significantly enhanced light-matter interaction, resulting in rapid and accurate alcohol concentration measurements. This makes the MC-PCF sensor a valuable tool for applications in industrial quality control, medical diagnostics, and environmental monitoring. Its superior sensitivity and low confinement loss underscore its potential as a reliable and efficient solution for alcohol detection across multiple fields.

#### Ethical Statement

This study does not contain any studies with human or animal subjects performed by any of the authors.

#### Conflicts of Interest

The authors declare that they have no conflicts of interest to this work.

#### Data Availability Statement

Data are available from the corresponding author upon reasonable request.

#### Author Contribution Statement

**Amit Halder:** Conceptualization, Methodology, Investigation, Writing – original draft, Writing – review & editing, Visualization. **Md Riyad Tanshen:** Software, Validation, Formal analysis, Resources, Data curation, Project administration. **Md Mushfiqur**

**Rahman Neidhe:** Investigation, Data curation, Writing – review & editing, Visualization. **Md Mohsin:** Methodology, Formal analysis, Supervision.

#### References

- [1] Dincer, C., Bruch, R., Costa-Rama, E., Fernández-Abedul, M. T., Merkoçi, A., Manz, A., . . . , & Güder, F. (2019). Disposable sensors in diagnostics, food, and environmental monitoring. *Advanced Materials*, 31(30), 1806739. <https://doi.org/10.1002/adma.201806739>
- [2] Niu, Z., Zhang, W., Yu, C., Zhang, J., & Wen, Y. (2018). Recent advances in biological sample preparation methods coupled with chromatography, spectrometry and electrochemistry analysis techniques. *TrAC Trends in Analytical Chemistry*, 102, 123–146. <https://doi.org/10.1016/j.trac.2018.02.005>
- [3] Pendão, C., & Silva, I. (2022). Optical fiber sensors and sensing networks: Overview of the main principles and applications. *Sensors*, 22(19), 7554. <https://doi.org/10.3390/s22197554>
- [4] Hu, D. J. J., Xu, Z., & Shum, P. P. (2019). Review on photonic crystal fibers with hybrid guiding mechanisms. *IEEE Access*, 7, 67469–67482. <https://doi.org/10.1109/access.2019.2917892>
- [5] Portosi, V., Laneve, D., Falconi, M. C., & Prudenzano, F. (2019). Advances on photonic crystal fiber sensors and applications. *Sensors*, 19(8), 1892. <https://doi.org/10.3390/s19081892>
- [6] Yu, R., Chen, Y., Shui, L., & Xiao, L. (2020). Hollow-core photonic crystal fiber gas sensing. *Sensors*, 20(10), 2996. <https://doi.org/10.3390/s20102996>
- [7] Islam, M. S., Sultana, J., Dinovitsler, A., Ahmed, K., Islam, M. R., Faisal, M., . . . , & Abbott, D. (2017). A novel Zeonex based photonic sensor for alcohol detection in beverages. In *2017 IEEE International Conference on Telecommunications and Photonics*, 114–118. <https://doi.org/10.1109/ictp.2017.8285905>
- [8] Islam, M. S., Paul, B. K., Ahmed, K., Asaduzzaman, S., Islam, M. I., Chowdhury, S., . . . , & Bahar, A. N. (2018).

- Liquid-infiltrated photonic crystal fiber for sensing purpose: Design and analysis. *Alexandria Engineering Journal*, 57(3), 1459–1466. <https://doi.org/10.1016/j.aej.2017.03.015>
- [9] Rahman, M. M., Mou, F. A., Al Mahmud, A., Bhuiyan, M. I. H., & Islam, M. R. (2019). Photonic crystal fiber based terahertz sensor for alcohol detection in beverages: Design and analysis. In *2019 IEEE International Conference on Telecommunications and Photonics*, 1–4. <https://doi.org/10.1109/ictp48844.2019.9041767>
- [10] Habib, M. A., Anower, M. S., AlGhamdi, A., Faragallah, O. S., Eid, M. M. A., & Rashed, A. N. Z. (2021). Efficient way for detection of alcohols using hollow core photonic crystal fiber sensor. *Optical Review*, 28(4), 383–392. <https://doi.org/10.1007/s10043-021-00672-6>
- [11] Shi, A. C., Maida, A. M., Shamsuddin, N., Kalam, M. A., & Begum, F. (2023). Photonic crystal fibre sensor for alcohol detection with extremely low birefringence. *International Journal of Applied Science and Engineering*, 20(2), 2022178. [https://doi.org/10.6703/ijase.202306\\_20\(2\).001](https://doi.org/10.6703/ijase.202306_20(2).001)
- [12] Das, D., Singh, A. K., Mandal, K. K., Funston, A. M., & Kumar, A. (2024). Unraveling the role of plasmonics in gold nanoparticle-integrated tapered fiber platforms for sensing applications. *Journal of Optical Microsystems*, 4(4), 041405. <https://doi.org/10.1117/1.JOM.4.4.041405>
- [13] Liang, W., Huang, Y., Xu, Y., Lee, R. K., & Yariv, A. (2005). Highly sensitive fiber Bragg grating refractive index sensors. *Applied Physics Letters*, 86(15), 151122. <https://doi.org/10.1063/1.1904716>
- [14] Halder, A., Tanshen, M. R., Akter, M. S., & Hossain, M. A. (2023). Design of highly birefringence and nonlinear modified honeycomb lattice photonic crystal fiber (MHL-PCF) for broadband dispersion compensation in E+S+C+L communication bands. *Engineering Proceedings*, 56(1), 19. <https://doi.org/10.3390/asec2023-15234>
- [15] Li, D., Zhang, W., Liu, H., Hu, J., & Zhou, G. (2017). High sensitivity refractive index sensor based on multicoating photonic crystal fiber with surface plasmon resonance at near-infrared wavelength. *IEEE Photonics Journal*, 9(2), 1–8. <https://doi.org/10.1109/jphot.2017.2687121>
- [16] Chang, H. J., Munera, N., Lopez-Zelaya, C., Banerjee, D., Beadie, G., van Stryland, E. W., & Hagan, D. J. (2024). Refractive index measurements of liquids from 0.5 to 2  $\mu\text{m}$  using Rayleigh interferometry. *Optical Materials Express*, 14(5), 1253–1267. <https://doi.org/10.1364/ome.519907>
- [17] Moutzouris, K., Papamichael, M., Betsis, S. C., Stavarakas, I., Hloupis, G., & Triantis, D. (2014). Refractive, dispersive and thermo-optic properties of twelve organic solvents in the visible and near-infrared. *Applied Physics B*, 116(3), 617–622. <https://doi.org/10.1007/s00340-013-5744-3>
- [18] Yuan, L., & Hu, Q. (2018). Comparisons of three kinds of plane wave methods for the Helmholtz equation and time-harmonic Maxwell equations with complex wave numbers. *Journal of Computational and Applied Mathematics*, 344, 323–345. <https://doi.org/10.1016/j.cam.2018.05.024>
- [19] Arosa, Y., & de la Fuente, R. (2020). Refractive index spectroscopy and material dispersion in fused silica glass. *Optics Letters*, 45(15), 4268–4271. <https://doi.org/10.1364/ol.395510>
- [20] Halder, A., & Anower, M. S. (2019). Relative dispersion slope matched highly birefringent and highly nonlinear dispersion compensating hybrid photonic crystal fiber. *Photonics and Nanostructures: Fundamentals and Applications*, 35, 100704. <https://doi.org/10.1016/j.photonics.2019.100704>
- [21] Singh, S., Upadhyay, A., Sharma, D., & Taya, S. A. (2022). A comprehensive study of large negative dispersion and highly nonlinear perforated core PCF: Theoretical insight. *Physica Scripta*, 97(6), 065504. <https://doi.org/10.1088/1402-4896/ac6d1a>
- [22] Kaur, V., & Singh, S. (2017). Extremely sensitive multiple sensing ring PCF sensor for lower indexed chemical detection. *Sensing and Bio-Sensing Research*, 15, 12–16. <https://doi.org/10.1016/j.sbsr.2017.05.001>
- [23] Danlard, I., Mensah, I. O., & Akowuah, E. K. (2022). Design and numerical analysis of a fractal cladding PCF-based plasmonic sensor for refractive index, temperature, and magnetic field. *Optik*, 258, 168893. <https://doi.org/10.1016/j.ijleo.2022.168893>
- [24] Nyachionjeka, K., Tarus, H., & Langat, K. (2020). Design of a photonic crystal fiber for optical communications application. *Scientific African*, 9, e00511. <https://doi.org/10.1016/j.sciaf.2020.e00511>
- [25] Olyae, S., & Taghipour, F. (2012). Ultra-flattened dispersion hexagonal photonic crystal fibre with low confinement loss and large effective area. *IET Optoelectronics*, 6(2), 82–87. <https://doi.org/10.1049/iet-opt.2011.0031>
- [26] Manickam, P., Senthil, R., & Senthil, R. (2024). Numerical analysis of hybrid: SPR-PCF multi-analyte sensor for clinical diagnosis. *Plasmonics*. Advance online publication. <https://doi.org/10.1007/s11468-024-02486-z>
- [27] Elabdein, M. Z., Khedr, O. E., Mohammed, N. A., & El-Rabaie, E. S. M. (2024). Recent advances in photonic crystal fiber based chemical and industrial sensors: A review. *Journal of Optics*. Advance online publication. <https://doi.org/10.1007/s12596-024-02218-w>
- [28] Sawraj, S., Kumar, D., Pravesh, R., Chaudhary, V. S., Pandey, B. P., Sharma, S., & Kumar, S. (2024). PCF-based sensors for biomedical applications—A review. *IEEE Transactions on NanoBioscience*. Advance online publication. <https://doi.org/10.1109/tmb.2024.3462748>

**How to Cite:** Halder, A., Tanshen, M. R., Neidhe, M. M. R., & Mohsin, M. (2025). Ultra-sensitive Photonic Crystal Fiber Based Refractive Index Sensor for Efficient Alcohol Detection at Near Infrared Region. *Journal of Optics and Photonics Research*. <https://doi.org/10.47852/bonviewJOPR52024904>